Communications in Nonlinear Science and Numerical Simulation 119 (2023) 107112

Contents lists available at ScienceDirect

Communications in Nonlinear Science and Numerical Simulation

journal homepage: www.elsevier.com/locate/cnsns

Research paper

A robust common-weights WENO scheme based on the flux vector splitting for Euler equations

Yiqing Shen [a,b,*], Shiyao Li [a,b], Shengping Liu [c], Kai Cui [a,b], Guannan Zheng [a,b,*]

[a] LHD, Institute of Mechanics, Chinese Academy of Sciences, Beijing 100190, China
[b] School of Engineering Science, University of Chinese Academy of Sciences, Beijing 100049, China
[c] Institute of Applied Physics and Computational Mathematics, Beijing 100094, China

ARTICLE INFO

Article history:
Received 27 September 2022
Received in revised form 8 December 2022
Accepted 5 January 2023
Available online 9 January 2023

Keywords:
Weighted essentially non-oscillatory scheme
Common-weights
Computational efficiency
Euler equations

ABSTRACT

This paper proposes a common-weights weighted essentially non-oscillatory (*Co-WENO*) scheme for solving the Euler equations of gas dynamics. Different from the usual component-wise weighting methods, common-weights means that, on one global stencil, a set of weights is commonly shared by the split flux vector of Euler equations in one spatial dimension. The common-weights WENO scheme has two significant advantages. First, since only one set of weights is calculated and used for the split flux vector, the method has an improved computational efficiency. Second, for a stencil (or each cell on the stencil), the Co-WENO scheme keeps the same contribution on each component numerical flux in a hyperbolic system of equations. How to calculate the weights is one of the vital issues in developing this kind of Co-WENO schemes.

In this paper, based on the flux vector split method, the product of density, pressure, and the split flux of energy equation($\Gamma^{\pm} = \rho p f_E^{\pm}$) is proposed to calculate the common weights. This is based on the following considerations: (1) the density jumps at shocks and contact discontinuities; (2) the split energy flux contains the term of the third power of the velocity (for example, u^3) and makes the resulting scheme has upwind characteristic; (3) the pressure always jumps at shocks, and it can help improve the stability in high speed flows, in which the kinetic energy is much larger than the internal energy. Numerical experiments also show that the proposed common-weights WENO scheme has good robustness and low numerical dissipation, and it can help suppress phase errors.

© 2023 Elsevier B.V. All rights reserved.

1. Introduction

Essentially non-oscillatory (*ENO*) and weighted essentially non-oscillatory (*WENO*) schemes have been developed for problems containing both discontinuities and piecewise smooth solutions. They have revolutionized the solution of nonlinear hyperbolic conservation laws, particularly for the Euler equations, which are often used as an inviscid approximation of the Navier–Stokes equations [1,2].

WENO schemes are based on ENO schemes [3,4]. Instead of choosing the smoothest stencil from candidate stencils, the WENO scheme uses a convex combination of all stencils. The WENO scheme was first proposed by Liu et al. [5] and then improved by Jiang and Shu [6]. After then, WENO schemes have been attracted a lot of attentions in CFD community.

* Corresponding author at: LHD, Institute of Mechanics, Chinese Academy of Sciences, Beijing 100190, China.
E-mail addresses: yqshen@imech.ac.cn (Y. Shen), zhengguannan@imech.ac.cn (G. Zheng).

https://doi.org/10.1016/j.cnsns.2023.107112
1007-5704/© 2023 Elsevier B.V. All rights reserved.

Balsara and Shu [7] extended the WENO schemes up to 11th-order of accuracy. Gerolymos et al. [5] further developed very-high-order WENO schemes. Henrick et al. [8] derived the necessary and sufficient conditions on the weights for fifth-order convergence of a fifth-order WENO scheme and proposed WENO-M scheme. Borges et al. [9] introduced a global smoothness indicator of higher-order and constructed WENO-Z scheme. Castro et al. [10] developed higher-order WENO-Z schemes. In order to obtain higher-order accuracy at critical points, various improved WENO-Z-type schemes [11–16]were suggested in recent years. Different from improving the accuracy of fifth-order WENO schemes at critical points, Shen et al. [17] developed a multistep WENO scheme to improve the accuracy at transition points. Ma et al. [18] and Zeng et al. [19] further improved multistep WENO schemes.

When a WENO scheme is applied to solve hyperbolic systems of equations, the WENO implementation is usually performed to reconstruct each of the characteristic variables (and hence the projections between the characteristic fields and the component space are needed), or each of the conservative variables, or directly construct the numerical flux of each split flux of the equations. From the viewpoint of computational efficiency, the characteristic variable reconstruction method is the most expensive one. In the early work of Jiang and Shu [6], to save the cost of computing the nonlinear weights and local characteristic decompositions, Jiang and Shu suggested using pressure to calculate the weights in the genuinely nonlinear characteristic fields and using entropy for the linearly degenerate fields. Numerical results showed that these replacements are effective at least for problems without strong shocks and reflective waves [6].

Compared to the characteristic variable reconstruction, the conservative variable reconstruction and the flux version of WENO method are simpler and more efficient. However, the two latter methods for equations may generate some spurious numerical issues. Johnsen [20] found that, when a finite volume formulation with the Lax–Friedrichs solver is used to solve problems with contact discontinuities, velocity and pressure oscillations are induced when high-order WENO reconstruction is performed directly on the conservative variables. Johnsen's analysis [20] showed that the weights used to calculate the conservative variables $(\rho, \rho u, E)$ are different, so that the reconstructed density has a different value in each equation and, as a result, an error is introduced in the velocity and pressure. To overcome these errors, the density must be reconstructed consistently in the mass, momentum and energy equations.

He et al. [21] analyzed the finite difference WENO schemes with the flux vector splitting (*FVS*) method and showed that the velocity and pressure oscillations near contact discontinuities are due to the incompatibility of the point-wise splitting of eigenvalues in FVS and the inconsistency of component-wise nonlinear difference discretization among equations of mass, momentum, energy, and even fluid compositions for multi-material flows. He et al. suggested combining a global FVS with a consistent discretization between different equations to suppress these oscillations. In the method of He et al. first, the smooth-factors for equations of mass and energy, and fluid compositions, but exclude the momentum equation, are calculated; then, the equation with the maximal value of smooth-factors is selected to calculate one set of common weights to weight all equations. The numerical results of He et al. and also our numerical results in this paper show that the method of He et al. can suppress the velocity and pressure oscillations near contact discontinuities, but it cannot eliminate the density oscillations that may come from the intrinsic nonlinear mechanism of a WENO scheme [21,22], and it is not so robust for some problems. In addition, since at least two smooth-factors are calculated, the method of He et al. seems not time-saving.

The purpose of the present paper is to develop high efficiency and robustness common-weights WENO (*Co-WENO*) scheme for Euler equations. First, since the global Lax–Friedrichs FVS is one of the most dissipative splitting methods [23], our method is based on the Steger–Warming FVS [24]. Then, the product of density, pressure, and the split flux of energy equation($\Gamma^{\pm} = \rho p f_E^{\pm}$) is proposed to calculate the common weights. This is based on the following considerations: (1) the density jumps at shocks and contact discontinuities; (2) the split energy flux contains the term of the third power of the velocity (for example, u^3) and makes the resulting scheme has upwind characteristic; (3) the pressure always jumps at shocks, and it can help improve the stability in high speed flows, in which the kinetic energy is much larger than the internal energy. Since only one set of weights is calculated and used for all equations, the method has high computational efficiency. Numerical experiments also show that the proposed common-weights WENO scheme has good robustness and low numerical dissipation, and it can effectively suppress phase errors.

This article is organized as follows: Section 2 introduces the WENO schemes for scalar conservation law equation. Section 3 presents the flux vector splitting methods and the common-weights WENO schemes for Euler equations, including the present method. Numerical experiments of one- and two-dimensional Euler problems are presented in Section 4. Conclusions are drawn in Section 5.

2. WENO schemes for scalar conservation law equation

For convenience, the one-dimensional scalar conservative law equation is used as a model to describe a numerical method

$$\frac{\partial u}{\partial t} + \frac{\partial f(u)}{\partial x} = 0. \tag{1}$$

The flux function $f(u)$ can be split into two parts as $f(u) = f^+(u) + f^-(u)$ with $df^+(u)/du \geq 0$ and $df^-(u)/du \leq 0$. By defining the points $x_i = i\Delta x$, $(i = 0, \ldots, N)$, where Δx is the uniform grid spacing, the semi-discrete of Eq. (1) can be written as

$$\frac{du_i}{dt} = -\frac{\hat{f}_{i+1/2} - \hat{f}_{i-1/2}}{\Delta x}, \tag{2}$$

where $\hat{f}_{i\pm1/2} = \hat{f}^{+}_{i\pm1/2} + \hat{f}^{-}_{i\pm1/2}$ is the numerical flux. In this paper, only the positive part $\hat{f}^{+}_{i+1/2}$ is described and the superscript '+' is dropped for simplicity. The flux $\hat{f}^{-}_{i+1/2}$ is evaluated following the symmetric rule about $x_{i+1/2}$.

2.1. The WENO-JS scheme

The numerical flux of a fifth-order WENO [6] scheme can be written as

$$\hat{f}_{i+1/2} = \sum_{k=0}^{2} \omega_k q_k, \tag{3}$$

where q_k is the third-order flux on the sub-stencil $S^3_k = (i+k-2, i+k-1, i+k)$, and given by

$$\begin{cases} q_0 = & \frac{1}{3}f_{i-2} - \frac{7}{6}f_{i-1} + \frac{11}{6}f_i, \\ q_1 = & -\frac{1}{6}f_{i-1} + \frac{5}{6}f_i + \frac{1}{3}f_{i+1}, \\ q_2 = & \frac{1}{3}f_i + \frac{5}{6}f_{i+1} - \frac{1}{6}f_{i+2}. \end{cases} \tag{4}$$

The weight ω_k of Jiang and Shu [6] is calculated as

$$\omega_k = \frac{\alpha_k}{\alpha_0+\alpha_1+\alpha_2}, \quad \alpha_k = \frac{c_k}{(IS_k+\epsilon)^2}, k = 0, 1, 2, \tag{5}$$

where, IS_k is called local smoothness indicator (*LSI*), which is used to measure the relative smoothness of a solution on the sub-stencil S_k. Constants $c_0 = 0.1, c_1 = 0.6$ and $c_2 = 0.3$ are the optimal weights, which generate the fifth-order upstream scheme. The parameter ϵ is a positive real number introduced to avoid the denominator becoming zero, and $\epsilon = 10^{-6}$ is suggested by Jiang and Shu [6].

In [6], Jiang and Shu proposed a classical local smoothness indicator (*LSI*) as

$$IS_k = \sum_{l=1}^{r-1} \int_{x_{i-1/2}}^{x_{i+1/2}} (\Delta x)^{2l-1} (q_k^{(l)})^2 dx, \tag{6}$$

where, $q_k^{(l)}$ is the lth order derivative of $q_k(x)$, and $q_k(x)$ is the interpolation polynomial on sub-stencil S^3_k.

For the fifth-order WENO scheme ($r = 3$), Eq. (6) gives

$$\begin{cases} IS_0 = \frac{13}{12}(f_{i-2} - 2f_{i-1} + f_i)^2 + \frac{1}{4}(f_{i-2} - 4f_{i-1} + 3f_i)^2, \\ IS_1 = \frac{13}{12}(f_{i-1} - 2f_i + f_{i+1})^2 + \frac{1}{4}(f_{i-1} - f_{i+1})^2, \\ IS_2 = \frac{13}{12}(f_i - 2f_{i+1} + f_{i+2})^2 + \frac{1}{4}(3f_i - 4f_{i+1} + f_{i+2})^2. \end{cases} \tag{7}$$

There are many methods proposed to improve the performance of WENO-JS, for example, WENO-M [8] was proposed by using a mapped function to increase the approximation of ω_k to the optimal weights c_k at critical points, WENO-Z [9] was proposed by introducing a global smoothness indicator to calculate the weights and hence has less dissipation and higher resolution than WENO-JS, Multi-step WENO [17] was constructed to improve the accuracy at transition points.

3. Flux vector splitting methods and common-weights WENO schemes for Euler equations

The one-dimensional Euler equations are taken as an example to describe the WENO schemes for the governing equations of gas dynamics,

$$\frac{\partial \mathbf{U}}{\partial t} + \frac{\partial \mathbf{F}}{\partial x} = 0, \tag{8}$$

$$\mathbf{U} = \begin{bmatrix} \rho \\ \rho u \\ E \end{bmatrix}, \ \mathbf{F} = \begin{bmatrix} \rho u \\ \rho u^2 + p \\ (E+p)u \end{bmatrix}, \tag{9}$$

and the equation of state is

$$p = (\gamma - 1)(E - \frac{1}{2}\rho u^2), \tag{10}$$

where ρ, u, E and p are density, velocity, total energy and pressure, respectively, γ is the ratio of specific heat. By using the conservative variable $\mathbf{U} = (u_1, u_2, u_3)^T$, the flux $\mathbf{F}$ can be written as

$$\mathbf{F}(\mathbf{U}) = \begin{bmatrix} u_2 \\ (\gamma-1)u_3 + \frac{3-\gamma}{2}\frac{u_2^2}{u_1} \\ \gamma\frac{u_2u_3}{u_1} - \frac{\gamma-1}{2}\frac{u_2^3}{u_1^2} \end{bmatrix}. \tag{11}$$

According to the hyperbolic character of the Euler system, there are

$$\mathbf{F} = \mathbf{A}U, \ \mathbf{A} = \frac{\partial F}{\partial U}, \ \mathbf{A} = \mathbf{R}\Lambda\mathbf{L}, \tag{12}$$

where, Λ is the diagonal matrix of the eigenvalues of the Jacobian matrix $\mathbf{A}$, $\Lambda = \mathrm{diag}(\lambda_1, \lambda_2, \lambda_3) = \mathrm{diag}(u, u-c, u+c)$, $c = \sqrt{\gamma p/\rho}$ is the speed of sound, and $\mathbf{R}$ and $\mathbf{L}$ are the matrices of the right and left eigenvectors, respectively. For convenience, here we give the formulations of the matrices $\mathbf{A}$, $\mathbf{R}$ and $\mathbf{L}$,

$$\mathbf{A} = \begin{bmatrix} 0 & 1 & 0 \\ \frac{\gamma-3}{2}u^2 & (3-\gamma)u & \gamma-1 \\ \frac{\gamma-1}{2}u^3 - uH & H-(\gamma-1)u^2 & \gamma u \end{bmatrix}, \ \mathbf{R} = \begin{bmatrix} 1 & 1 & 1 \\ u & u-c & u+c \\ \frac{1}{2}u^2 & H-uc & H+uc \end{bmatrix},$$

$$\mathbf{L} = \mathbf{R}^{-1} = \begin{bmatrix} 1-\frac{\gamma-1}{2c^2}u^2 & \frac{\gamma-1}{c^2}u & -\frac{\gamma-1}{c^2} \\ \frac{1}{2}\left(\frac{\gamma-1}{2c^2}u^2 + \frac{u}{c}\right) & -\frac{1}{2}\left(\frac{\gamma-1}{c^2}u + \frac{1}{c}\right) & \frac{\gamma-1}{2c^2} \\ \frac{1}{2}\left(\frac{\gamma-1}{2c^2}u^2 - \frac{u}{c}\right) & -\frac{1}{2}\left(\frac{\gamma-1}{c^2}u - \frac{1}{c}\right) & \frac{\gamma-1}{2c^2} \end{bmatrix},$$

with the enthalpy $H = (E+p)/\rho$.

3.1. The flux vector splitting methods for Euler equations

The flux $\mathbf{F}$ can be split into positive and negative parts as $\mathbf{F} = \mathbf{F}^+ + \mathbf{F}^-$,

$$\mathbf{F}^\pm = \mathbf{A}^\pm U, \quad \mathbf{A}^\pm = \mathbf{R}\Lambda^\pm\mathbf{L}, \tag{13}$$

where the eigenvalues matrices $\Lambda^+ = \mathrm{diag}(\lambda_1^+, \lambda_2^+, \lambda_3^+)$ and $\Lambda^- = \mathrm{diag}(\lambda_1^-, \lambda_2^-, \lambda_3^-)$ with $\lambda_j^+ \geq 0, \lambda_j^- \leq 0 (j = 1, 2, 3)$, and $\Lambda = \Lambda^+ + \Lambda^-$.

The generalized formulations of the split fluxes can be written as

$$\mathbf{F}^\pm = \begin{bmatrix} f_1^\pm \\ f_2^\pm \\ f_3^\pm \end{bmatrix} = \frac{\rho}{2\gamma}\begin{bmatrix} 2(\gamma-1)\lambda_1^\pm + \lambda_2^\pm + \lambda_3^\pm \\ 2(\gamma-1)\lambda_1^\pm u + \lambda_2^\pm(u-c) + \lambda_3^\pm(u+c) \\ (\gamma-1)\lambda_1^\pm u^2 + \frac{\lambda_2^\pm}{2}(u-c)^2 + \frac{\lambda_3^\pm}{2}(u+c)^2 + w \end{bmatrix}, \tag{14}$$

where,

$$w = \frac{(3-\gamma)(\lambda_2^\pm + \lambda_3^\pm)c^2}{2(\gamma-1)}.$$

There are many methods to carry out Eq. (13). For example, in the Steger–Warming (SW) flux vector splitting method [24], the eigenvalues are calculated as

$$\lambda_j^\pm = \frac{1}{2}(\lambda_j \pm |\lambda_j|), \tag{15}$$

the global Lax–Friedrichs (GLF) splitting method [25] takes

$$\lambda_j^\pm = \frac{1}{2}(\lambda_j \pm \alpha), \tag{16}$$

where α is the maximal eigenvalue over the whole computational domain.

Clearly, the global Lax–Friedrichs splitting method has a simple form as

$$\mathbf{F}^\pm = \begin{bmatrix} f_1^\pm \\ f_2^\pm \\ f_3^\pm \end{bmatrix} = \frac{1}{2}\begin{bmatrix} \rho u \pm \alpha\rho \\ \rho u^2 + p \pm \alpha\rho u \\ (E+p)u \pm \alpha E \end{bmatrix}. \tag{17}$$

Similar to the scalar case, the semi-discrete form of Eq. (8) can be written as

$$\frac{dU_{l,i}}{dt} = -\frac{\hat{f}_{l,i+1/2} - \hat{f}_{l,i-1/2}}{\Delta x}, \tag{18}$$

and $\hat{f}_{l,i\pm1/2} = \hat{f}^+_{l,i\pm1/2} + \hat{f}^-_{l,i\pm1/2}$. Traditionally, if a component-wise WENO scheme is applied, the numerical flux $\hat{f}_{l,i\pm1/2}$ (specifically the weights $\omega_{l,k}$) is calculated independently by the lth component-wise flux $f_l^\pm (l = 1, 2, 3)$.

3.2. The method of He et al. for solving contact discontinuities

He et al. [21] analyzed the finite difference WENO schemes with the flux vector splitting (FVS) method for the Euler equations and showed that the velocity and pressure oscillations near contact discontinuities may be caused by either one of the incompatibility of the point-wise splitting of eigenvalues in FVS and the inconsistency of component-wise nonlinear difference discretization among equations of mass, momentum, energy, and even fluid composition for multi-material flows. Hence, He et al. suggested using the global Lax–Friedrichs FVS to avoid the incompatibility of the point-wise splitting of eigenvalues in FVS, and developing common-weights methods to guarantee consistent discretization between different equations.

In Ref. [21], the common weights of numerical fluxes $\hat{f}_{l,i+1/2}(l = 1, 2, 3)$ are determined as follows:

(1) Split the flux **F** into positive and negative parts by using the global Lax–Friedrichs splitting method Eq. (17).

(2) Calculate the smoothness factor β_l for the lth split flux (only the split fluxes of mass- and energy-equations are suggested by He et al. hence, l takes only 1 and 3 for the 1D Euler equations).

$$\beta_l = \frac{\sum_{k=0}^{2}(IS_{k,l} + \epsilon)}{min(IS_{0,l}, \ldots, IS_{2,l} + \epsilon)}, \tag{19}$$

where ϵ is an adaptive number calculated by the primary ϵ-adaptivity technique [22],

$$\epsilon = \begin{cases} \epsilon_{max}, & \tau_5 \le S_{min}, \\ \epsilon_{min}, & \tau_5 \ge S_{max}, \\ \dfrac{\epsilon_{min} - \epsilon_{max}}{S_{max} - S_{min}}(\tau_5 - S_{min}) + \epsilon_{max}, & otherwise, \end{cases} \tag{20}$$

where $\epsilon_{min} = 10^{-6}$, $\epsilon_{max} = 10^{-2}$, $S_{min} = 10^{-3}$, and $S_{max} = 10^{-1}$. $\tau_5 = |IS_{0,l} - IS_{2,l}|$ is the fifth-order global smoothness indicators introduced in WENO-Z schemes [9].

(3) Select the equation with the maximal value of β_l (denoted with l_0) and use its smoothness indicators IS_{k,l_0} to calculate the common weights ω_k.

There are many methods to calculate the unnormalized nonlinear weights, the formulation of WENO-JS [6] is used in [21]

$$\alpha_k = \frac{c_k}{(IS_{k,l_0} + \epsilon)^2}, \quad k = 0, 1, 2. \tag{21}$$

Using α_k, one can obtain the normalized weights ω_k Eq. (5). Then, the final weighted fluxes for all equations are calculated as

$$\hat{f}_{l,i+1/2} = \omega_0 q_{l,0} + \omega_1 q_{l,1} + \omega_2 q_{l,2}, \quad l = 1, 2, 3, \tag{22}$$

where, l denotes the lth equation in Euler system. $q_{l,k}$ ($k = 0, 1, 2$) is the kth candidate flux (see Eq. (4)) on the sub-stencil S_k^3.

3.3. The new common-weights WENO scheme for Euler equations

The new method is motivated by the following analysis:

(1) As mentioned above, the method of He et al. needs to calculate two sets of smoothness indicators to estimate the smooth factors and to select the final equation to calculate the common weights. If we can find one available variable to calculate only one set of smoothness indicators and also the common weights, the computational efficiency can be improved. Besides, there are several empirical parameters introduced in Eq. (20). This may result in the method cannot work well for some problems. For example, since $\tau_5 = |IS_{0,l} - IS_{2,l}|$ is related with the dimension of flux f, if different reference values are used to nondimensionlize f, then those values of parameters S_{min} and S_{max} may become ineffective.

Moreover, from the formula of the total energy E

$$E = \frac{p}{\gamma - 1} + \frac{1}{2}\rho u^2,$$

it can be seen that, if $p \ll \rho u^2$, there is

$$E \sim \frac{1}{2}\rho u^2.$$

Hence, applying the first or last equation of Eq. (17) to calculate the common weights may not reasonably reflect the pressure jumps and possibly generate negative pressure. This may be part of the reasons for the decreased robustness of traditional WENO schemes and also the method of He et al. for solving some extreme cases.

(2) The numerical results of He et al. and also our numerical results in this paper show that the method can suppress the velocity and pressure oscillations near contact discontinuities, but it cannot eliminate the density oscillation that may come from the intrinsic nonlinear mechanism of a WENO scheme [21,22].

(3) Gressier et al. [26] proved that if a FVS scheme exactly preserves stationary contact discontinuities, then it cannot be positively conservative.

(4) The global Lax–Friedrichs FVS is known to be the most diffusive [1].

Hence, in this paper, we focus on developing a robust common-weights WENO (*Co-WENO*) scheme for Euler equations based on the Steger–Warming flux vector splitting method and find that the product of density, pressure, and the split flux of energy equation can serve as the variable to calculate the common weights. This is also based on the following considerations:

(1) the density jumps at shocks and contact discontinuities;

(2) the split energy flux contains the term of the third power of the velocity (for example, u^3) and makes the resulting scheme has the upwind characteristic;

(3) the pressure always jumps at shocks, and it can help improve the stability in high speed flows, in which the kinetic energy is much larger than the internal energy.

That is, the serving variable is designed as

$$\Gamma^{\pm}(i) = \rho(i)p(i)f_E^{\pm}(i), \tag{23}$$

where, $f_E^{\pm}(i)$ is the split energy flux of Steger–Warming FVS method (for example, $f_E^{\pm}(i)$ is $f_3^{\pm}(i)$ in Eq. (15) for 1D Euler equations).

Here is the fifth-order Co-WENO algorithm for the 1D Euler equations:

(1) Split the flux vector by Eq. (14) and get

$$\Gamma^{\pm}(i) = \rho(i)p(i)f_E^{\pm}(i).$$

(2) Calculate the common weights (for brevity, only the positive part is given and the superscript '+' is dropped)

$$\begin{aligned}
IS_0 &= \frac{13}{12}(\Gamma_{i-2} - 2\Gamma_{i-1} + \Gamma_i)^2 + \frac{1}{4}(\Gamma_{i-2} - 4\Gamma_{i-1} + 3\Gamma_i)^2,\\
IS_1 &= \frac{13}{12}(\Gamma_{i-1} - 2\Gamma_i + \Gamma_{i+1})^2 + \frac{1}{4}(\Gamma_{i-1} - \Gamma_{i+1})^2,\\
IS_2 &= \frac{13}{12}(\Gamma_i - 2\Gamma_{i+1} + \Gamma_{i+2})^2 + \frac{1}{4}(3\Gamma_i - 4\Gamma_{i+1} + \Gamma_{i+2})^2,\\
\alpha_k &= \frac{c_k}{(IS_k + \epsilon)^2}, \quad k = 0, 1, 2, \quad !WENO - JS\\
\omega_k &= \frac{\alpha_k}{\alpha_0 + \alpha_1 + \alpha_2}, \quad k = 0, 1, 2.
\end{aligned}$$

(3) Calculate the numerical fluxes

$$\begin{aligned}
&DO\ l = 1, 3 \quad !for\ 1D\ Euler\ equations\\
&\quad q_0 = \frac{1}{3}f_{l,i-2} - \frac{7}{6}f_{l,i-1} + \frac{11}{6}f_{l,i},\\
&\quad q_1 = -\frac{1}{6}f_{l,i-1} + \frac{5}{6}f_{l,i} + \frac{1}{3}f_{l,i+1},\\
&\quad q_2 = \frac{1}{3}f_{l,i} + \frac{5}{6}f_{l,i+1} - \frac{1}{6}f_{l,i+2},\\
&\quad \hat{f}_{l,i+1/2} = \omega_0 q_0 + \omega_1 q_1 + \omega_2 q_2.\\
&ENDDO
\end{aligned}$$

The un-normalized weights α_k can be calculated by different schemes, for example, by using the WENO-Z scheme, there is

$$\alpha_k = c_k\left(1 + \frac{\tau_5}{IS_k + \epsilon}\right), \quad \tau_5 = |IS_0 - IS_2|, \quad k = 0, 1, 2. \tag{24}$$

4. Numerical examples

In this paper, the semi-discretized ordinary differential equations of Euler equations are solved by the third-order total variation diminishing (*TVD*) Runge–Kutta method [4]

$$\begin{aligned}
U^{(1)} &= U^n + \Delta t L(U^n),\\
U^{(2)} &= \tfrac{3}{4}U^n + \tfrac{1}{4}U^{(1)} + \tfrac{1}{4}\Delta t L(U^{(1)}),\\
U^{n+1} &= \tfrac{1}{3}U^n + \tfrac{2}{3}U^{(2)} + \tfrac{2}{3}\Delta t L(U^{(2)}),
\end{aligned} \tag{25}$$

where L is the spatial operator, U^n is the solution at time step n.

To compare the new method and the method of He et al. all the numerical examples in this paper are calculated by using the formulation (21) of WENO-JS, which is used by He et al. [21]. The serving variable and the common-weights

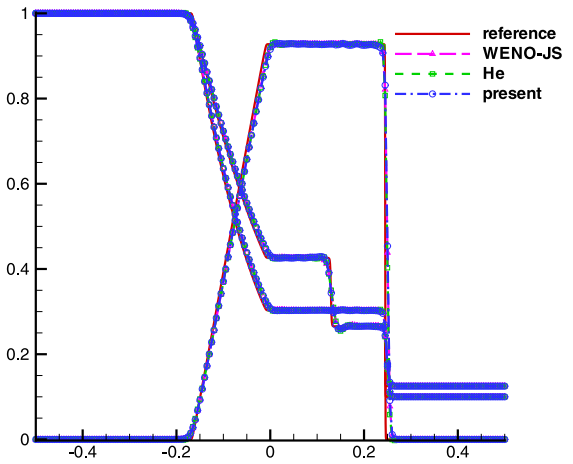

Fig. 1. Sod problem, N = 200.

idea are also effective for other weighting methods, for brevity, this paper only gives several 1D results calculated by using the formulation (24) of WENO-Z.

4.1. One-dimensional Euler problems

For the one-dimensional problems, the time step is taken as

$$\Delta t = \frac{\sigma \Delta x}{max_i \left(|u_i| + c_i\right)}, \tag{26}$$

where, $\sigma = 0.5$ is CFL number, c is the speed of sound. For all 1D cases in this paper, the reference solutions are obtained by WENO-JS with characteristic-wise reconstruction [6] and $N = 2000$.

4.1.1. Case 1

The Sod shock tube problem is taken as the first case of one-dimensional Euler problems to compare different schemes. The initial condition is

$$(\rho, u, p) = \begin{cases} (1.0, 0.0, 1.0), & x \le 0.5, \\ (0.125, 0.0, 0.1), & x > 0.5. \end{cases} \tag{27}$$

Figs. 1 and 2 give the numerical results with $N = 200$ at $T = 1.4$. It can be seen that, near the contact discontinuity, the method of He et al. (for convenience, we call it He-method in the following context)can suppress the pressure and velocity oscillations, but it cannot prevent the density oscillation (lower part of Fig. 2). In addition, near both the expansion and shock waves, the velocity oscillations produced by He-method are more obvious (upper part of Fig. 2). Developing effective FVS methods to resolve both the shock waves and contact discontinuities is still an open issue.

The results also showed that, though the proposed common-weights method cannot avoid the numerical oscillations of contact discontinuities, it is available for solving Euler equations as the traditional component-wise weighting method.

4.1.2. Case 2

The second 1-D case is the Shu–Osher problem [4] with the initial condition

$$(\rho, u, p) = \begin{cases} (3.857143,\ 2.629369,\ 31/3) & -5 \le x < -4, \\ (1 + 0.2\sin(5x),\ 0,\ 1) & -4 \le x \le 5. \end{cases} \tag{28}$$

Figs. 3 and 4 give the distributions of density at $t = 1.8$ by using $N = 200$ and $N = 300$. As these figures showed, for this kind of high-frequency problem, since the Steger–Warming splitting method is less dissipative than the global L-F splitting method, the results of WENO-JS and the present scheme are more accurate than the He-method. We also can see that the present common-weights WENO method has the least numerical dissipation, and it seems effective to suppress phase errors.

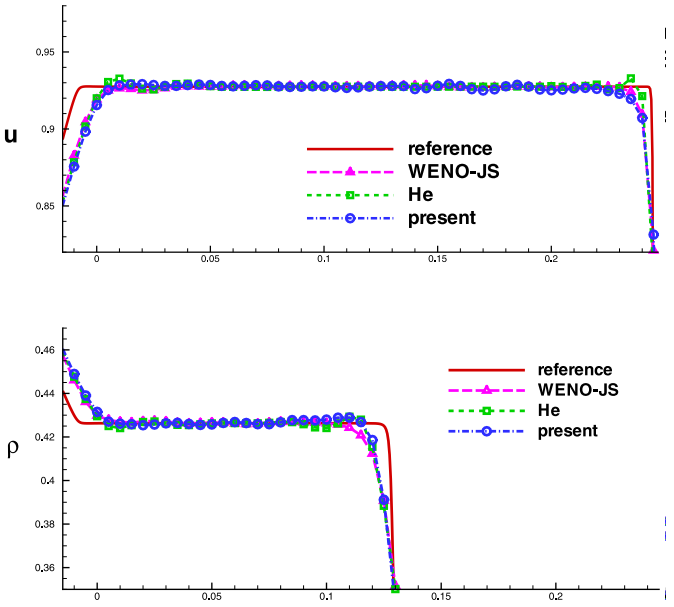

Fig. 2. Enlarged plot of Fig. 1.

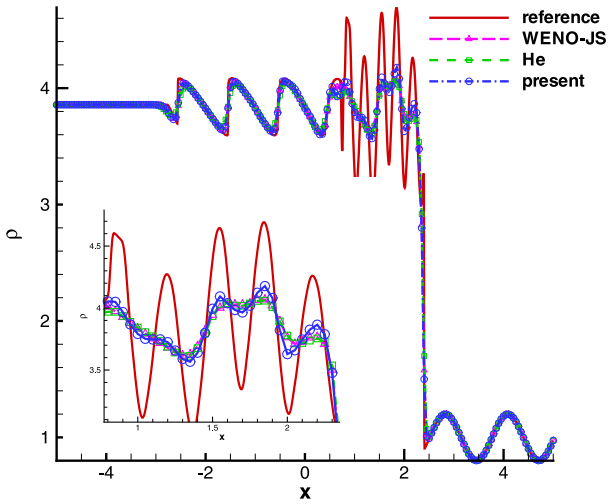

Fig. 3. Density distribution of Shu–Osher problem, N = 200.

4.1.3. Case 3

The third case is the interactive blast waves problem [9] with the initial condition

$$(\rho, u, p) = \begin{cases} (1,\ 0,\ 1000) & 0 \le x < 0.1, \\ (1,\ 0,\ 0.001) & 0.1 \le x < 0.9, \\ (1,\ 0,\ 100) & 0.9 \le x \le 1. \end{cases} \tag{29}$$

The numerical results at $t = 0.038$ with $N = 400$ and $N = 600$ are presented in Figs. 5 and 6. With $N = 400$, at the first peak (near $x = 0.65$), the He-method looks better than the other two schemes, but it becomes more dissipative at the second peak (near $x = 0.8$). With $N = 600$, the He-method shows abnormal behaviors near $x = 6.3$ and $x = 0.7$. Near the peaks and valley, the He-method is more dissipative than both WENO-JS and the present method.

To validate the common-weights idea can be available to other improved WENO schemes, the above three cases are also calculated by using the weighting formulation (24) of WENO-Z. The results of the common-weights WENO-Z is denoted as Co-WENO-Z. Figs. 7–9 show that the serving variable (23) and the common-weights idea are effective for the WENO-Z

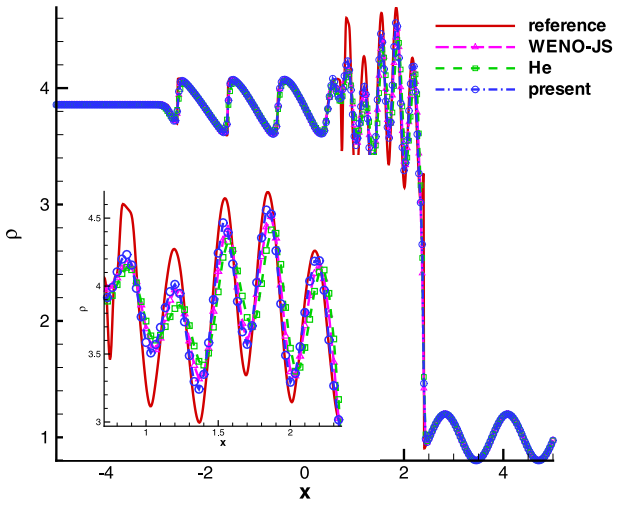

Fig. 4. Density distribution of Shu–Osher problem, N = 300.

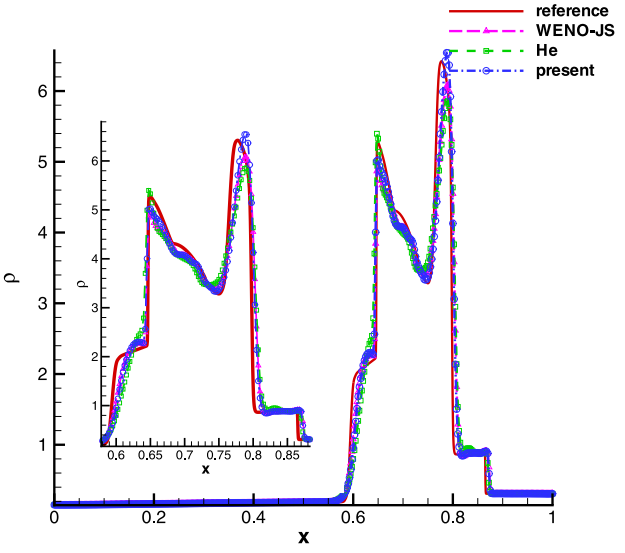

Fig. 5. Density distribution of interactive blast waves, N = 400.

method. In particular, for the high frequency wave (Fig. 8) and the interactive blast waves problem (Figs. 9 and 10), Co-WENO-Z obtains more accurate solutions than the traditional component-wise WENO-Z scheme.

4.2. Two-dimensional Euler equations

The two-dimensional Euler equations can be written as

$$\frac{\partial U}{\partial t}+\frac{\partial F}{\partial x}+\frac{\partial G}{\partial y}=0, \tag{30}$$

where the conservative variables U, the inviscid flux vectors F and G are

$$U=\begin{bmatrix}\rho\\ \rho u\\ \rho v\\ E\end{bmatrix},\ F=\begin{bmatrix}\rho u\\ \rho u^2+p\\ \rho uv\\ Eu+pu\end{bmatrix},\ G=\begin{bmatrix}\rho v\\ \rho uv\\ \rho v^2+p\\ Ev+pv\end{bmatrix}. \tag{31}$$

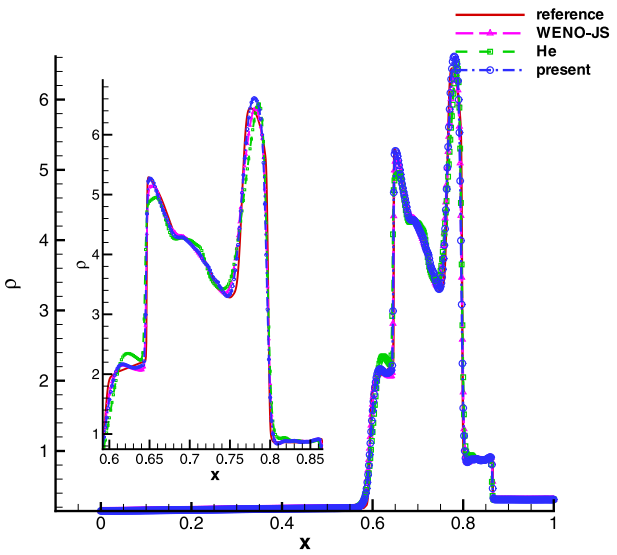

Fig. 6. Density distribution of interactive blast waves, N = 600.

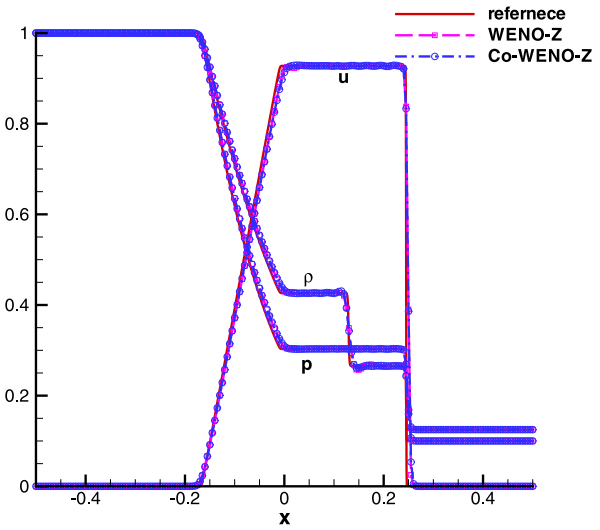

Fig. 7. Sod problem, WENO-Z, N = 200.

where

$$p = (\gamma - 1)(E - \frac{\rho}{2}(u^2 + v^2)). \tag{32}$$

The time step is taken as follows [27]:

$$\Delta t = \delta \frac{\Delta t_x \Delta t_y}{\Delta t_x + \Delta t_y}, \ with \ \Delta t_x = \frac{\Delta x}{max_{i,j}(|u_{i,j}| + c_{i,j})}, \ \Delta t_y = \frac{\Delta y}{max_{i,j}(|v_{i,j}| + c_{i,j})}, \tag{33}$$

where $\delta = 0.5$ is the CFL number.

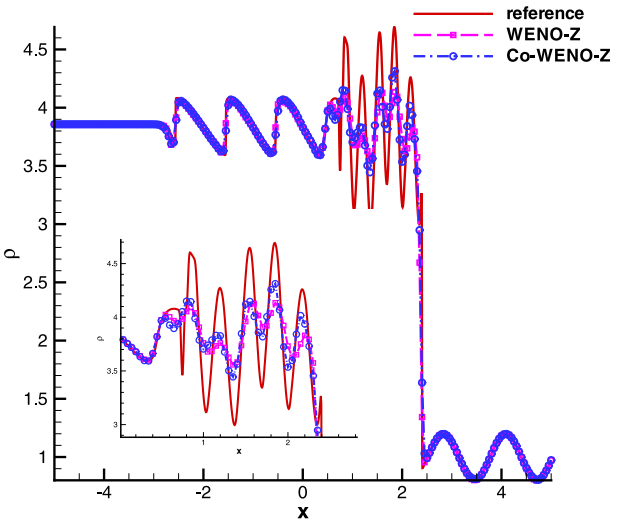

Fig. 8. Density distribution of Shu-Osher problem, WENO-Z N = 200.

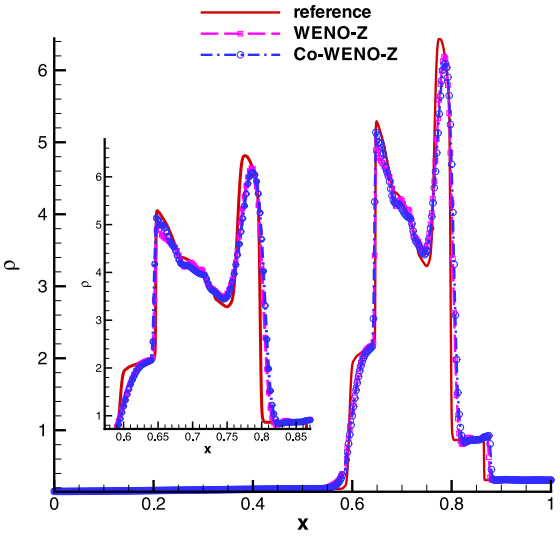

Fig. 9. Interactive blast waves, WENO-Z, N = 400.

4.2.1. Case 4

This first two-dimensional case is a Riemann configuration [11,28] with the initial conditions

$$(\rho, u, v, p) = \begin{cases} (1.5,\ 0,\ 0,\ 1.5) & 0.8 \le x \le 1, 0.8 \le y \le 1, \\ (0.5323,\ 1.206,\ 0,\ 0.3) & 0 \le x < 0.8, 0.8 \le y \le 1, \\ (0.138,\ 1.206,\ 1.206,\ 0.029) & 0 \le x < 0.8, 0 \le y < 0.8, \\ (0.5323,\ 0,\ 1.206,\ 0.3) & 0.8 \le x \le 1, 0 \le y < 0.8. \end{cases} \tag{34}$$

The mesh of 400 × 400 is used. The density contours at $t = 0.8$ are shown in Figs. 11. It can be seen that three schemes can capture reflection shocks and contact discontinuities well. But the present scheme can resolve the roll-up of the Kelvin-Helmholtz instability with finer structures than the others.

Table 1 gives the CPU-time comparison of different schemes (Fortran code). It can be seen that, for the 2D case, the present Co-WENO scheme can save about 16% CPU time of WENO-JS. The He-method with the global Lax–Friedrichs FVS can save 19% CPU time of WENO-JS with the Steger–Warming FVS. The main reason is that the global Lax–Friedrichs FVS is simpler and hence computational cheaper than the Steger–Warming FVS. If the He-method is applied with the Steger–Warming FVS, it is even more expensive than WENO-JS. This is because two smooth factors (19) for equations of mass and energy are needed to calculate.

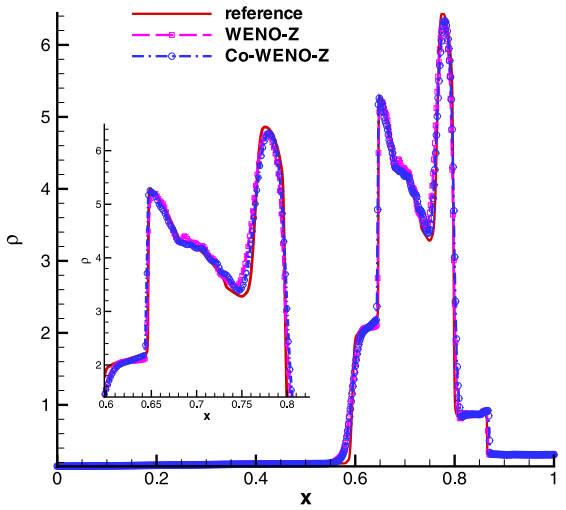

Fig. 10. Interactive blast waves, WENO-Z, N = 600.

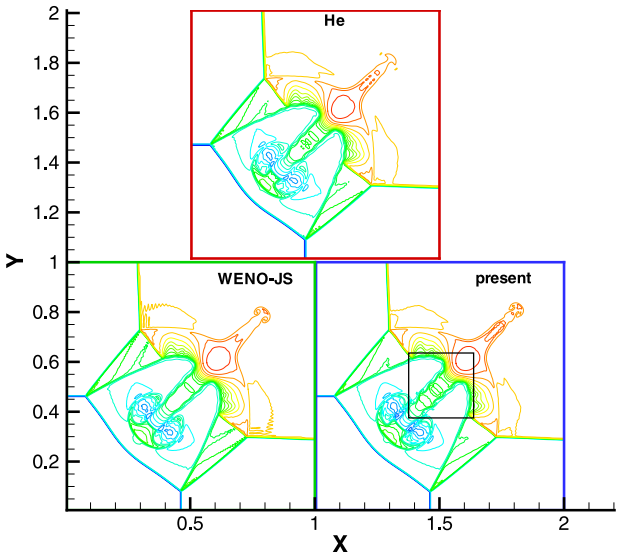

Fig. 11. Density contours with 400 × 400 grid.

Table 1
CPU-time comparison of different schemes.

	WENO-JS (SW)	He-method (GLF)	Co-WENO (present, SW)	He-method (SW)
CPU-time (s)	421	343	355	446
Efficiency	1.00	0.81	0.84	1.06

4.2.2. Case 5

The two-dimensional Rayleigh–Taylor instability problem [29,30] is often used to test the numerical dissipation of a high-order scheme. It describes the interface instability between fluids with different densities when acceleration is directed from heavy fluid to light one. The gravitational effect is introduced by adding ρ and ρv to the flux of the y-momentum and the energy equations, respectively. The initial distribution is

$$(\rho, u, v, p) = \begin{cases} (2, 0, -0.025\alpha\cos(8\pi x), 2y + 1), & 0 \le y < 1/2, \\ (1, 0, -0.025\alpha\cos(8\pi x), y + 3/2), & 1/2 \le y < 1, \end{cases} \tag{35}$$

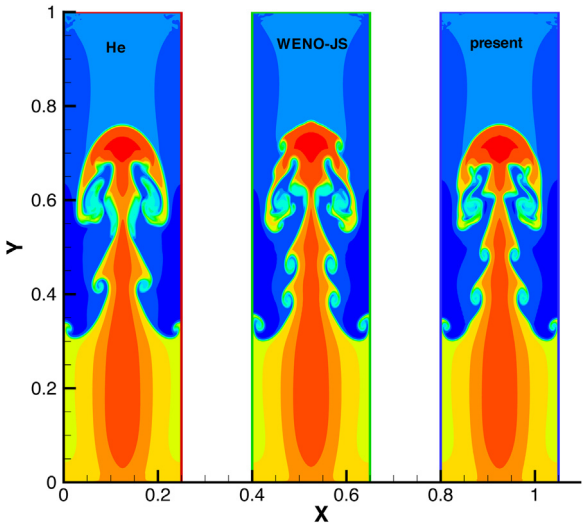

Fig. 12. Density contours with 240 × 960 grid.

and $\alpha = \sqrt{\gamma p/\rho}$ is the speed of sound with $\gamma = 5/3$. The computational domain is $[0, 0.25] \times [0, 1]$. The left and right boundaries are reflective boundary conditions, and the top and bottom boundaries are set as $(\rho, u, v, p) = (1, 0, 0, 2.5)$ and $(\rho, u, v, p) = (2, 0, 0, 1)$, respectively.

The solution at $t = 1.95$ is solved with mesh of 240 × 960 grid points. The density contours are plotted in Fig. 12. As observed in 1D cases, due to less dissipation, the WENO-JS and the present schemes generate more complex unstable structures than the He-method.

4.2.3. Case 6

A two-dimensional shock vortex interaction problem is solved to further demonstrate the high resolution of the present scheme. The problem is taken from Jiang and Shu [6]. It describes the interaction between a stationary shock and a vortex. The computational domain is taken to be $[0, 2] \times [0, 1]$. A stationary Mach 1.1 shock is positioned at $x = 0.5$ and normal to the x-axis. Its left state is $(\rho, u, v, p) = (1, 1.1\sqrt{\gamma}, 0, 1)$. A small vortex is superimposed to the flow on the left of the shock and is centered at $(x_c, y_c) = (0.25, 0.5)$. The vortex is described as a perturbation to the velocity (u, v), temperature $(T = p/\rho)$, and entropy $(S = ln(p/\rho^{\gamma}))$ of the mean flow and denoted by the tilde values:

$$\tilde{u} = \varepsilon\tau e^{a(1-\tau^2)} sin\theta,$$

$$\tilde{v} = -\varepsilon\tau e^{a(1-\tau^2)} cos\theta,$$

$$\tilde{T} = -\frac{(\gamma-1)\varepsilon^2 e^{2a(1-\gamma^2)}}{4a\gamma},$$

$$\tilde{S} = 0,$$

where $\tau = r/r_c$ and $r = \sqrt{(x-x_c)^2 + (y-y_c)^2}$, ε indicates the strength of the vortex, a controls the decay rate of the vortex, and r_c is the critical radius for which the vortex has the maximum strength. As in Ref. [6], $\varepsilon = 0.3$, $r_c = 0.05$, and $a = 0.204$ are adopted in this paper.

A mesh of 400 × 200 is used. Fig. 13 is the density contours at $t = 0.60$. Fig. 14 gives the comparisons of the density along the centerline of $y = 0.5$. To show the accuracy of the new scheme, the reference obtained by the WENO-JS scheme with a refined mesh of 2000 × 1000 is also given. It can be seen that the original He-method generates density oscillation near $x = 0.49$. And we also can see that the oscillation can be suppressed by using $\epsilon = 10^{-20}$ to replace the adaptive $\epsilon(20)$ suggested in [21]. Even though, at the peak and valley, the solutions obtained by the present scheme are still more accurate than those of the He-method and also the WENO-JS scheme. Similar as observed in the Shu–Osher shock tube problem, the present scheme can help suppress the phase error effectively.

4.2.4. Case 7

The Sedov blast wave problem [31] is a well known benchmark test to study a strong explosion problem. The initial conditions are given as follows,

$$(\rho, u, v, E) = \begin{cases} (1, 0, 0, 10^{-12}), & if\ x > \Delta x, y > \Delta y, \\ (1, 0, 0, \frac{0.244816}{\Delta x \Delta y}), & otherwise. \end{cases} \tag{36}$$

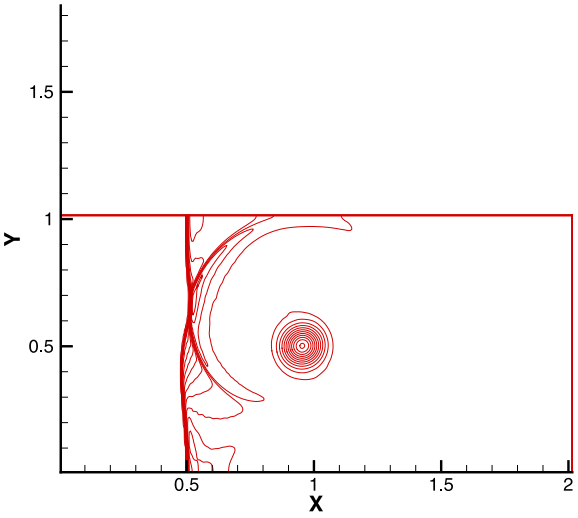

Fig. 13. Density contours of shock/vortex interaction by the present scheme, N = 400.

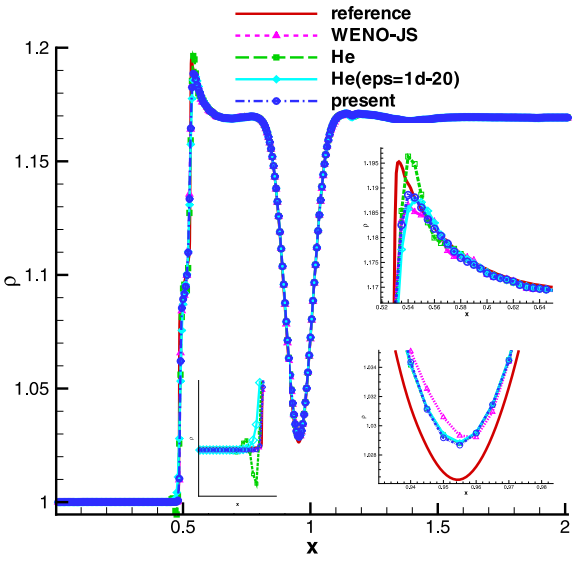

Fig. 14. Density distribution along the line of $y = 0.5$.

The computational domain is $[0, 1.1] \times [0, 1.1]$. The numerical boundary treatment is reflective for the left and bottom edges, zero-order extrapolation for the right and top edges. The density contours obtained by the present method with the mesh of 200×200 are given in Fig. 15. Fig. 16 is the density distribution along $y = 0$. For this problem, the computation of the He-method(regardless of the fixed value $\epsilon = 10^{-20}$ or the adaptive function ϵ Eq. (20) in [21]) blows up, and hence no result is obtained. The new method resolves the strong shock pretty well, and its shock profile is sharper than WENO-JS.

5. Conclusion remarks

This paper presents a common-weights WENO (Co-WENO) method for solving the Euler equations of gas dynamics.

(1) The common weights are calculated by using the product of the split flux of energy equation, density, and pressure.

(2) The Co-WENO scheme guarantees consistent discretization between different component equations of the Euler equations.

(3) Since only one set of weights is calculated, the method has high computational efficiency.

(4) Numerical experiments also show that the present Co-WENO scheme has good robustness and low numerical dissipation, and it can effectively suppress phase errors.

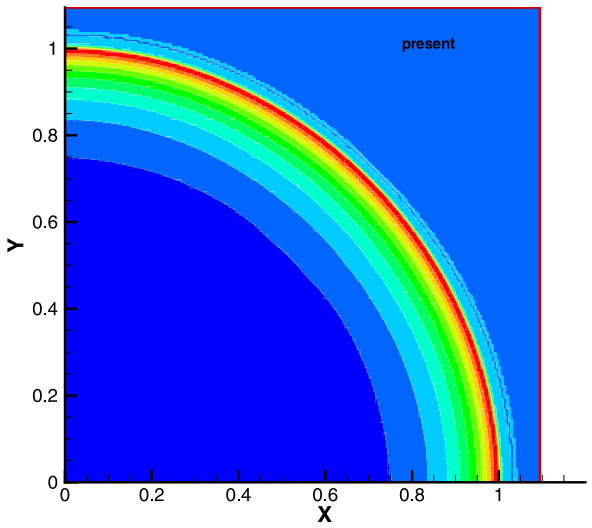

Fig. 15. Density contours of Sedov problem with 200 × 200, the present scheme.

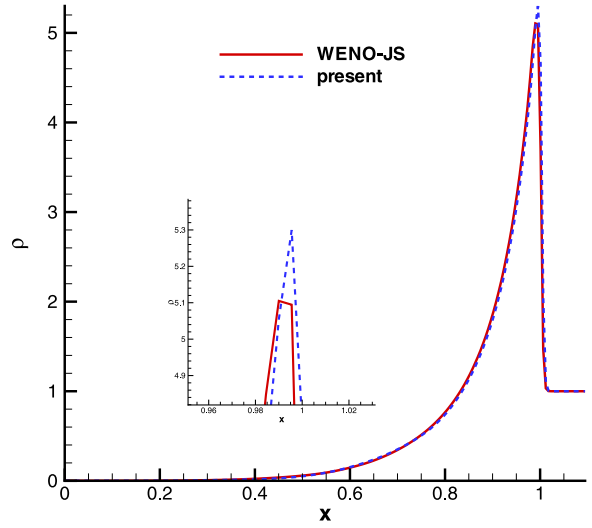

Fig. 16. Density distribution along $y = 0$.

(5) The common-weights method can be easily extended to other weighting methods, such as those of WENO-M and WENO-Z.

(6) The common-weights method of the variables reconstruction combined with the Riemann solvers, such as Roe scheme, HLL scheme, is in progress and will be presented in an upcoming paper.

CRediT authorship contribution statement

Yiqing Shen: Conceptualization, Methodology, Writing, Supervision. **Shiyao Li:** Validation. **Shengping Liu:** Validation. **Kai Cui:** Review & editing. **Guannan Zheng:** Validation, Resources, Review & editing.

Declaration of competing interest

The authors declare that they have no known competing financial interests or personal relationships that could have appeared to influence the work reported in this paper.

Data availability

Data will be made available on request.

Acknowledgments

This research work was supported by NSFC, China Nos. 11872067, 91852203, 11902326, and 12172364.

References

[1] Shu C-W. Essentially non-oscillatory and weighted essentially non-oscillatory schemes for hyperbolic conservation laws. ICASE Report No.97-65, 1997.
[2] Shu C-W. High order WENO and DG methods for time-dependent convection-dominated PDEs: A brief survey of several recent developments. J Comput Phys 2016;316:598–613.
[3] Harten A, Engquist B, Osher S, Chakravarthy SR. Uniformly high order accurate essentially non-oscillatory schemes, III. J Comput Phys 1987;71:231–303.
[4] Shu C-W, Osher S. Efficient implementation of essentially non-oscillatory shock-capturing schemes. J Comput Phys 1988;77:439–71.
[5] Liu X-D, Osher S, Chan T. Weighted essentially non-oscillatory schemes. J Comput Phys 1994;115:200–12.
[6] Jiang G-S, Shu C-W. Efficient implementation of weighted ENO schemes. J Comput Phys 1996;126:202–28.
[7] Balsara DS, Shu C-W. Monotonicity preserving weighted essentially non-oscillatory schemes with increasingly high order of accuracy. J Comput Phys 2000;160:405–52.
[8] Henrick AK, Aslam TD, Powers JM. Mapped weighted essentially non-oscillatory schemes: Achieving optimal order near critical points. J Comput Phys 2005;207:542–67.
[9] Borges R, Carmona M, Costa B, Don WS. An improved weighted essentially non-oscillatory scheme for hyperbolic conservation laws. J Comput Phys 2008;227:3191–211.
[10] Castro M, Costa B, Don WS. High order weighted essentially non-oscillatory WENO-Z schemes for hyperbolic conservation laws. J Comput Phys 2011;230:1766–92.
[11] Ha Y, Kim CH, Lee YJ, Yoon J. An improved weighted essentially non-oscillatory scheme with a new smoothness indicator. J Comput Phys 2013;232:68–86.
[12] Don WS, Borges R. Accuracy of the weighted essentially non-oscillatory conservative finite difference schemes. J Comput Phys 2013;250:347–72.
[13] Fan P, Shen YQ, Tian BL, Yang C. A new smoothness indicator for improving the weighted essentially non-oscillatory scheme. J Comput Phys 2014;269:329–54.
[14] Hu XY, Wang Q, Adams NA. An adaptive central-upwind weighted essentially non-oscillatory scheme. J Comput Phys 2010;229:8952–65.
[15] Acker F, de R. Borges RB, Costa B. An improved WENO-Z scheme. J Comput Phys 2016;313:726–53.
[16] Liu SP, Shen YQ, Zeng FJ, Yu M. A new weighting method for improving the WENO-Z scheme. Internat J Numer Methods Fluids 2018;87:271–91.
[17] Shen YQ, Liu L, Yang Y. Multistep weighted essentially non-oscillatory scheme. Internat J Numer Methods Fluids 2014;75:231–49.
[18] Ma YK, Yan ZG, Zhu HJ. Improvement of multistep WENO scheme and its extension to higher orders of accuracy. Internat J Numer Methods Fluids 2016;82:818–38.
[19] Zeng FJ, Shen YQ, Liu SP, Liu L. A high performance fifth-order multistep WENO scheme. Internat J Numer Methods Fluids 2019;91:159–82.
[20] Johnsen E. On the treatment of contact discontinuities using WENO schemes. J Comput Phys 2011;230:8665–8.
[21] He ZW, Zhang YS, Li XL, Li L, Tian BL. Preventing numerical oscillations in the flux-split based finite difference method for compressible flows with discontinuities. J Comput Phys 2015;300:269–87.
[22] Jia F-L, Gao Z, Don W-S. A spectral study on the dissipation and dispersion of the WENO schemes. J Sci Comput 2014;63:49–77.
[23] Nonomura T, Fujii K. Characteristic finite-difference WENO scheme for multicomponent compressible fluid analysis: Overestimated quasi-conservative formulation maintaining equilibriums of velocity, pressure, and temperature. J Comput Phys 2017;340:358–88.
[24] Steger JL, Warming RF. Flux vector splitting of the inviscid gasdynamic equations with application to finite-difference methods. J Comput Phys 1981;40:263–93.
[25] Shu C-W, Osher S. Efficient implementation of essentially non-oscillatory shock-capturing schemes, II. J Comput Phys 1989;83:32–78.
[26] Gressier J, Villedieu P, Moschetta JM. Positivity of flux vector splitting schemes. J Comput Phys 1999;155:199–220.
[27] Pirozzoli S. Conservative hybrid compact-WENO schemes for shock-turbulence interaction. J Comput Phys 2002;178:81–117.
[28] Balsara DS. Multidimensional HLLE Riemann solver: Application to Euler and magnetohydrodynamic flows. J Fluid Mech 2010;229:1970–93.
[29] Shi J, Zhang YT, Shu CW. Resolution of high order WENO schemes for complicated flow structures. J Comput Phys 2003;186:690–6.
[30] Yong YN, Tufo H, dubey A, Rosner R. On the miscible Rayleigh-Taylor instability: two and three dimensions. J Fluid Mech 2001;447:337–408.
[31] Sedov L. Similarity and dimensional methods in mechanics. New York, NY: Academic Press; 1959.